Design of a Modulated FSS Subreflector for a Dual-Reflector System

Michael F. Palvig and Min Zhou
TICRA
Copenhagen, Denmark
mz@ticra.com

***Abstract*—This paper describes the design of a modulated FSS subreflector for a S/Ka-band Cassegrain dual-reflector system. The FSS subreflector separates the radiation from the S-band (2.0-2.3 GHz) and Ka-band (25.5-2.7.5 GHz). To simplify the manufacturing of the subreflector, a conical FSS subreflector is considered. Instead of using a periodic FSS where all array elements are identical, a modulated FSS subreflector with varying sized array elements is considered. The FSS elements are optimized to emulate an axial displaced hyperboloid surface, thereby compensating for the non-optimal conical subreflector surface. In Ka-band, the optimized modulated FSS subreflector improves the peak gain of the antenna system with more 6 dBs compared to the use of a periodic FSS.**

***Index Terms*—satellite antennas, frequency selective surface, sub-reflector, dual-reflector antenna**

I. Introduction

Frequency Selective Surfaces (FSS) [1] have a long heritage and are widely used in various antenna systems. In particular reflector antenna configurations including at least one FSS subreflector have been used for decades for space applications such as exploration, Earth observation, data relay as well as in deep-space ground stations [2]–[7].

In many configurations, FSS subreflectors are planar structures, making them easy to manufacture. However, for certain antenna configurations, e.g., a Cassegrain dual-reflector system, the FSS subreflector is doubly-curved. Although FSS subreflectors have been successfully manufactured and used in space, the doubly-curved surface complicates the manufacturing process resulting in higher costs and risks. To ease the manufacturing process, simpler surface shapes are preferred, but this can entail degraded antenna performance.

In [8], a reflectarray is used as a planar subreflector in a Cassegrain dual-reflector system to compensate for surface distortions on the main reflector. Because of the phasing capabilities of a reflectarray [9], the array elements can be designed to compensate for the errors introduced by the main reflector surface distortions. The same concept can be applied for a FSS subreflector. Instead of having a periodic FSS subreflector where the array elements are periodically deployed onto the subreflector surface, a modulated FSS subreflector with varying sized array elements can compensate for surface errors on the main or subreflector. The idea bears resemblance to FSS-backed reflectarrays [10], [11]. But instead of optimizing the antenna to provide a pencil/shaped beam, the array elements are designed to compensate for certain surface errors.

Modulated FSS designs have been considered previously [12], [13], but not as a surface compensating FSS. In this paper, we present the design of a modulated FSS subreflector in a Cassegrain dual-reflector system. The subreflector has a conical shape and does not provide the optimal performance. The goal is to emulate an axial displaced hyperboloid surface with the conical FSS subreflector.

II. Antenna Configuration

For the antenna configuration, we consider a center-fed Cassegrain dual-reflector system as shown in Fig. 1. The antenna is a traditional combined S/Ka-band antenna with a FSS subreflector. The main reflector has a diameter of 2 m and the height of the antenna less than 0.75 m, hence it is a compact antenna system. The feeds below and above the subreflector are the Ka-band and S-band feeds, respectively. For simplicity, Gaussian beam patterns are considered for the feeds and struts are not included in the configuration. The requirements for the antenna are summarized in Table I.

Ideally, the subreflector has a hyperboloid surface. However, to facilitate easier manufacturing, a conical sub-reflector with a diameter of 0.28 m is considered. A conical surface is singly-curved, hence it is easier to manufacture compared to a hyperboloid surface which is doubly-curved. Despite the fact that the conical shape of the subreflector is defined to be as close to the ideal hyperboloid surface as possible, a large degradation in performance is observed. The peak gain of the antenna system with the hyperboloid is 54.9 dBi, whereas with the conical subreflector it is only 47.5 dBi, hence a degradation of more than 7 dB. We would like to compensate the performance degradation using a modulated FSS by shaping the reflected field from the subreflector.

TABLE I
Antenna Requirements

Frequency	Polarization	Peak Gain
$2.0 - 2.3$ GHz	RHCP	>30 dBi
$25.5 - 27.5$ GHz	RHCP	>54 dBi

III. Analysis and Optimization Methods

For the design of the modulated FSS, we apply the direct optimization design procedure that is adopted in the dedicated

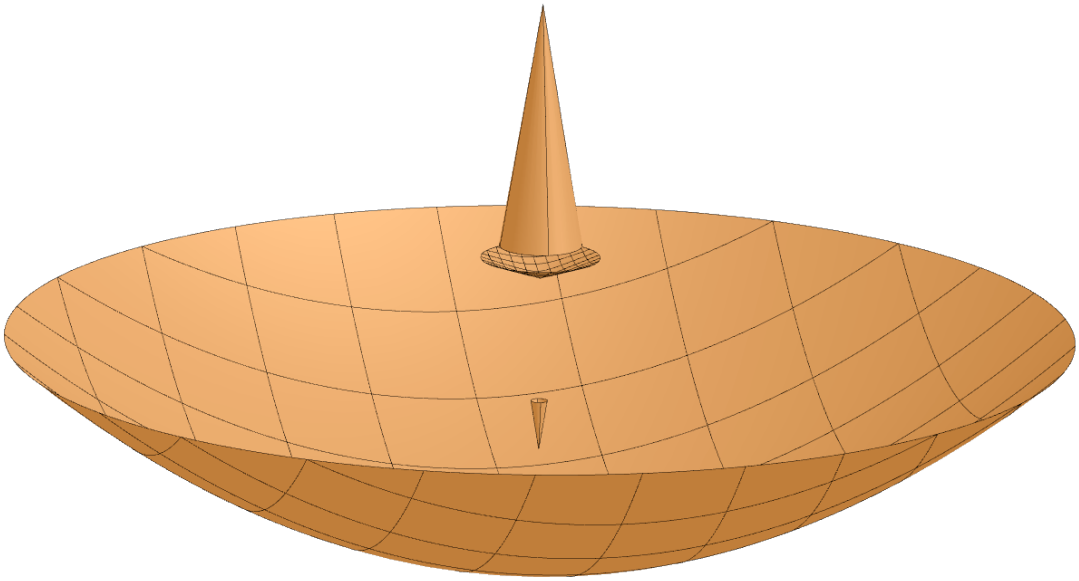

Fig. 1. Center-fed Cassegrain dual-reflector system with a conical subreflector and a paraboloidal main reflector. The feeds below and above the subreflector are the Ka-band and S-band horn, respectively.

software tool that TICRA has developed for the analysis and design of quasi-periodic surfaces, QUPES (short for QUasi-PEriodic Surfaces). In this approach, all the FSS elements are optimized simultaneously to directly fulfill the far-field requirements of the entire antenna system, which in our case is the radiation from the main reflector, the FSS subreflector, and the feed.

The analysis method in QUPES is a method of moments based method assuming local periodicity. Several optimization algorithm are available in QUPES, but we apply a gradient-based minmax algorithmn, which has proven to be provide good reflectarray designs [14].

For the design of the modulated FSS subreflector, the optimization variables would be the dimensions of the individual FSS elements. For large subreflector dimensions, the number of array elements can be large, hence also the number of optimization variables. For modulated FSS designs where we do not expect any rapid changes in the element geometry over the surface, it is convenient to describe the element variation using spline functions [12]. For a given geometrical parameter of the array element, a, the variation over the surface is expresed in terms of basis splines as function of the position

$$a(x,y) = \sum_{i}^{N_i} \sum_{j}^{N_i} c_{ij} B_i(x) B_j(y), \tag{1}$$

where c_{ij} is the spline coefficients, $B_i(x)$ and $B_j(y)$ are basis spline functions, and N_i and N_j are the number of spline functions in x and y, respectively. By varying c_{ij}, the modulation over the surface is varied.

In this way, it is possible to define the modulated FSS by adjusting a small number of spline function coefficients instead of the individual element dimensions. This results in a significantly reduced number of optimization variables when designing such surfaces.

This is particularly important when optimizing the array elements for secondary pattern performances, which is the case in the present application, where we are interested in the radiation from the main reflector. The reason for this is due to the calculation of the derivatives in the gradient-based optimization algorithm. For primary pattern performance optimization, e.g., reflectarray optimization where we are interested in the radiation directly from the array elements, the derivatives can be computed analytically. This means that the number of optimization variables can easily be greater than tens of tousands without compromising the optimization time. For secondary pattern performance optimization, the derivatives can not always be computed analytically, hence the computation increases significantly and it is important to keep the number of optimization variables low.

This feature is available in QUPES and is applied to our design here.

IV. FSS Element

The FSS must be reflective in the Ka-band range 25.5 GHz to 27.5 GHz and transmissive in the S-band range 2.0 GHz to 2.3 GHz. Further, for the shaping effect to work, the reflection phase in the Ka-band should be tunable across the elements.

There are basically two main FSS types to choose from: inclusion type and hole type. The former consists of inclusions

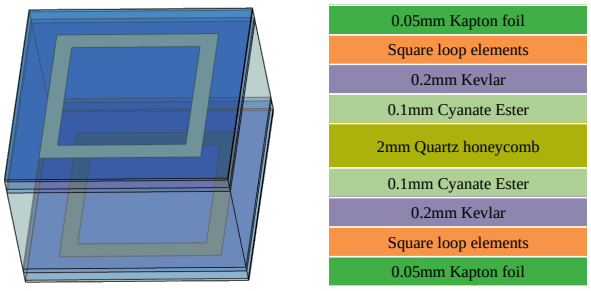

Fig. 2. The FSS unit cell topology consisting of two square loop element layers separated by dielectric substrates.

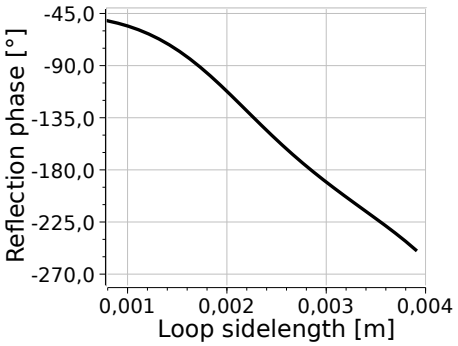

Fig. 3. The phase curve of the unit cell: Phase of the reflected wave as a function of the size of the loops on the face of incidence. The loop sidelength is varied from $0.8\,\mathrm{mm}$ to $3.9\,\mathrm{mm}$.

in a plane and is reflective when the inclusions resonate, otherwise transmissive. The latter consists of holes in a conductive screen and is transmissive when the holes resonate, otherwise reflective. The inclusion type is the appropriate choice here for two reasons: 1) The reflective band is at a higher frequency than the transmissive so if holes were used, they might have had higher order resonances in the reflective band, 2) to be able to tune the reflection phase, the elements must be near resonance at the reflection frequencies.

As for inclusion shape, the choice falls on a square loop. It is a fairly compact element, which exhibits quite wide tuning range. However, when we start changing the sizes of the square loops in order to vary the reflection phase, the reflectivity will degrade. Therefore, a second layer of square loops which are kept at resonance is placed beneath the variable ones, separated by layers of microwave substrates. The bottom layer of loops will act as a ground plane at Ka-band, and thus the structure will work as a reflectarray.

The unit cell topology is shown in Fig. 2. The detailed layer structure is inspired from [15]. The copper elements are etched on a Kapton foil layer. The Kapton layer is stiffened by a sandwich of Kevlar and Cyanate Ester. Finally, a Quartz honeycomb layer provides an appropriate RF separation. Refer to [15] for a more detailed justification of the material choices.

The unit cell dimensions are set to $4.0\,\mathrm{mm}$. For the reference designs without modulation (periodic) the loop sidelengths are fixed: $2.9\,\mathrm{mm}$ in the layer towards the main reflector and $2.91\,\mathrm{mm}$ in the layer facing away. This results in a reflection coefficient better than $-0.15\,\mathrm{dB}$ for incidence angles less than $30°$ (angle of cone) in the chosen Ka-band range. The corresponding transmission in the S-band is better than $-0.2\,\mathrm{dB}$.

In Fig. 3, we show the reflection phase when varying the loop size of the elements facing the incident wave (side facing the main reflector) at the center frequency of the Ka-band. It is observed that we can obtain a reflection phase range of approximately $200°$. For a general flat reflectarray design, a range of $360°$ is needed, such that any reflection phase can be synthesized. In the present case however, the surface that we are trying to emulate, the hyperboloid, is geometrically very close to the conical FSS, thus a phase range less than $360°$ is adaquete.

V. FSS Subreflector

A. FSS Design

As mentioned in Section II, the starting point of design is a conical FSS subreflector which is as close as possible to the original hyperboloid subreflector shape. This initial configuration does work, but the performance degradation is significant.

In order to improve the illumination of the main reflector, the loop sizes of the face closest to the main reflector are varied. As described in Section III, the elements are not individually changed, but their sizes follow a set of basis splines covering the surface. A higher number of basis splines supports a more complex variation of loop sizes accross the surface.

Though we talk about emulating a hyperboloid with the phase change of the FSS elements, this is not explicitly enforced. Most other works in the field of transmit- and reflectarrays, take the approach of mapping out the element dimensions based on the phase change needed to emulate a certain surface. In QUPES, the optimization instead targets the desired end result directly. This generally provides better overall designs, and gives the user endless flexibility in specifying the optimization goals to match project requirements. In the present case we have chosen just a single goal, namely to maximize the on-axis gain of the full dual-reflector system at Ka-band.

In this case, the optimzation time increases roughly linearly with the number of unknowns (spline functions). Therefore we start with a low number of spline functions and increase this number until we have a satisfactory result.

B. Results

Table II shows a summary of the achieved gain when optimizing with different numbers of spline functions to represent the element geometries. The gain using the hyperboloid subreflector is also shown as a reference result. It is seen that as more spline functions are added, the result obtained from the optimization improves. But when more than doubling the number of splines from 184 to 420, only $0.3\,\mathrm{dB}$ is

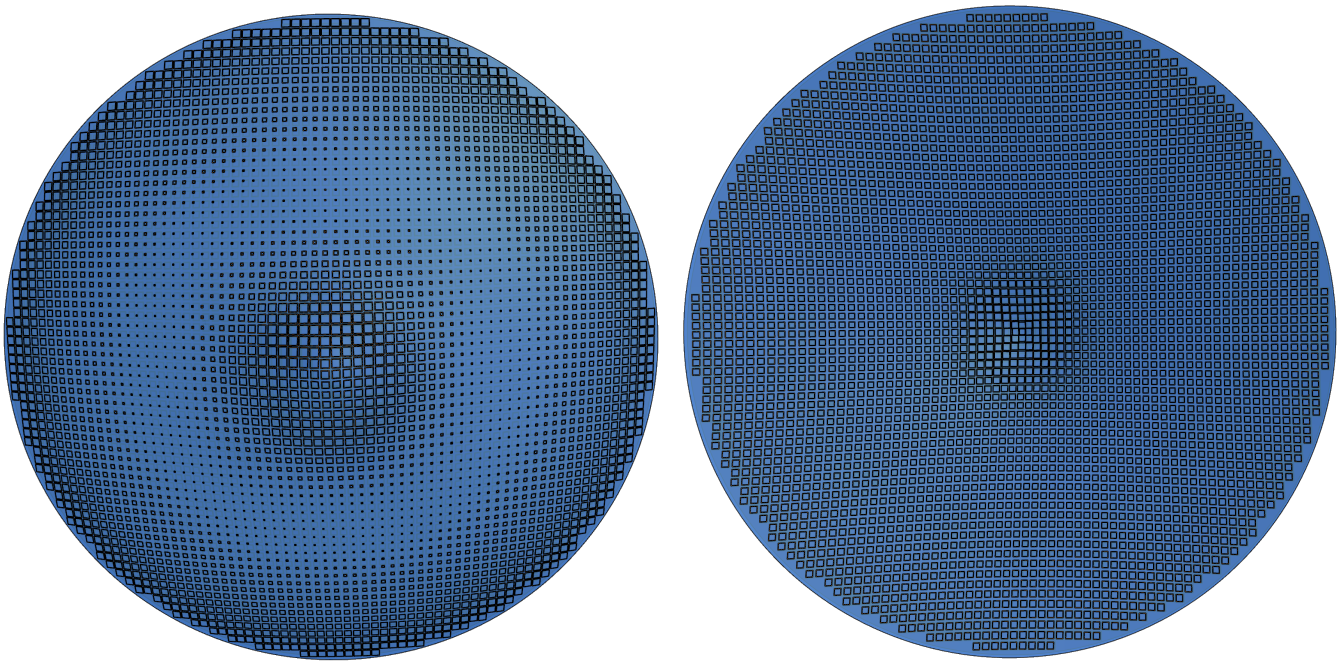

(a) (b)

Fig. 4. Element distribution on the conical modulated FSS, (a) side facing towards the main reflector, (b) side facing away from main reflector.

gained, which suggests that not much more performance can be extracted from this configuration. In the last entry, the elements on the other side of the FSS are also optimized. Only a very small improvement is achieved from this increase in complexity.

The element distributions on both sides of the best FSS design are shown in Fig. 4. It is seen that the elements on the side facing the main reflector varies significantly, shaping the reflected field to improve the illumination onto the main reflector. The elements on the side facing away from the main reflector do not vary much. This is expected, because if the elements shall act as a ground plane, they must be near resonance, otherwise they will let some of the Ka-band field through, thus degrading the overall gain.

The patterns in Ka- and S-bands are shown in Fig. 5 and Fig. 6, respectively. The hyperboloid FSS still exhibits better performance than the modulated conical FSS design. In the S-band, the conical FSS disturbs the S-band feed slightly more than the hyperboloid FSS does. The difference in gain between the hyperboloid FSS and the modulated conical FSS is $0.9\,\mathrm{dB}$ in the Ka-band and $0.3\,\mathrm{dB}$ in the S-band. This is the price to be paid for the simpler manufacturing of a single curved surface.

TABLE II
ACHIEVED RESULTS WITH DIFFERENT NUMBER OF SPLINE FUNCTIONS

FSS shape	Number of splines	Achieved gain
Hyperboloid	None	54.9 dB
Conical	None	47.5 dB
	16	49.1 dB
	36	51.0 dB
	81	52.6 dB
	184	53.7 dB
	420	54.0 dB
	840 (420 per layer)	54.1 dB

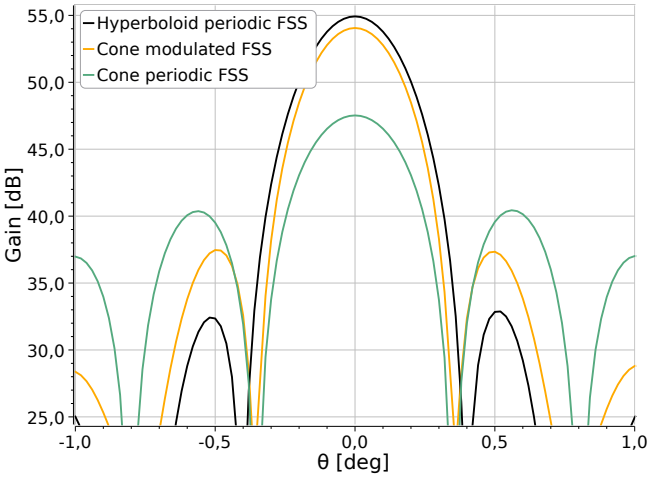

Fig. 5. Ka-band patterns of the modulated conical FSS shown in Fig. 4 compared with unmodulated conical and hyperboloid FSS. The patterns are plotted for the lowest frequency in the band, $25.5\,\mathrm{GHz}$, where all three configurations exhibit the lowest gain.

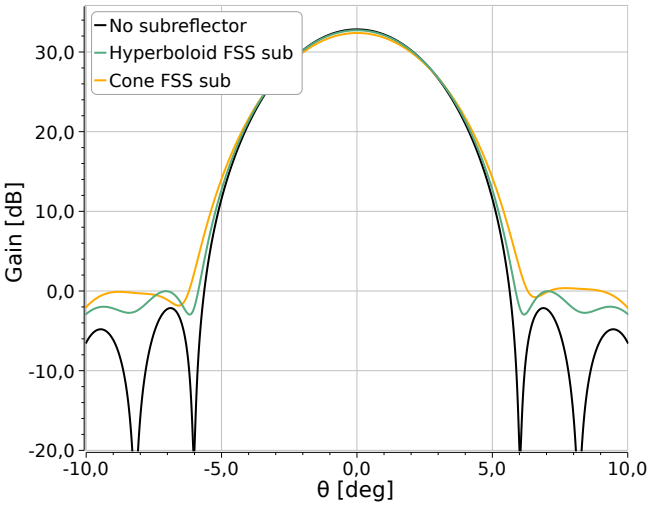

Fig. 6. S-band patterns without an FSS, with an unmodulated hyperboloid FSS, and with the conical modulated FSS shown in Fig. 4. The patterns are plotted for the lowest frequency in the band, 2.0 GHz, where all three configurations exhibit the lowest gain.

VI. Conclusion

We show in this paper that a modulated FSS can be used to compensate for surface errors such as non-optimal subreflector surface. This is demonstrated by considering a center-fed S/Ka-band Cassegrain dual-reflector antenna with an FSS subreflector that separates the radiation from the two bands. To ease the manufacturing of the FSS subreflector a conical subreflector is considered instead of a hyperboloid surface. This results in degraded performance because of the non-optimal illumination of the main reflector from the conical FSS. To compensate this, a modulated FSS design is employed and optimized to emulate the ideal hyperboloid surface. The FSS consists of two layers of square loop elements. Optimizing the size of the loop elements, it is possible to improve the gain of the antenna system using a periodic FSS subreflector from 47.5 dBi to 54.1 dBi, which is an improvement of more than 6 dB.

References

[1] T. K. Wu, *Frequency Selective Surface and Grid Array*. Wiley Interscience, 1995.

[2] T.-K. Wu, "Double-square-loop fss for multiplexing four (s/x/ku/ka) bands," in *Proc. IEEE AP-S Int. Symp. 1991*. IEEE, 1991, pp. 1885–1888.

[3] V. Agrawal and W. Imbriale, "Design of a dichroic cassegrain subreflector," *IEEE Trans. Antennas Propag.*, vol. 27, no. 4, pp. 466–473, 1979.

[4] R. Mizzoni, "The cassini high gain antenna (hga): a survey on electrical requirements, design and performance," in *Spacecraft Antennas, IEE/SEE Seminar on*. IET, 1994, pp. 6–1.

[5] R. Martin and D. Martin, "Quasi-optical antennas for radiometric remote-sensing," *Electronics & communication engineering journal*, vol. 8, no. 1, pp. 37–48, 1996.

[6] P. Ingvarson, F. S. Johansson, and L. E. Pettersson, "A dichroic subreflector for a communication satellite," in *Proc. IEEE AP-S Int. Symp. 1989*. IEEE, 1989, pp. 1088–1091.

[7] P. Besso, M. Bozzi, L. perregrini, L. S. Drioli, and W. Nickerson, "Deep-space antenna for Rosetta mission: design and testing of the S/X band dichroic mirror," *IEEE Trans. Antennas Propag.*, vol. 51, no. 3, pp. 388–394, 2003.

[8] H. Rajagopalan and Y. Rahmat-Samii, "Reflector surface distortion compensation using reflectarray: experimental verification," in *Proc. EuCap*, 2011.

[9] J. Huang and J. A. Encinar, *Reflectarray Antennas*. IEEE Press, 2008.

[10] J. Shaker, R. Chaharmir, and H. Legay, "Investigation of fss-backed reflectarray using different classes of cell elements," *IEEE Trans. Antennas Propag.*, vol. 56, no. 12, pp. 3700–3706, 2008.

[11] R. Deng, S. Xu, F. Yang, and M. Li, "An fss-backed ku/ka quad-band reflectarray antenna for satellite communications," *IEEE Trans. Antennas Propag.*, vol. 66, no. 8, pp. 4353–4358, 2018.

[12] M. Zhou, S. B. Sørensen, N. Vesterdal, R. Dickie, P. Baine, J. Montgomery, R. Cahill, M. Henry, P. G. Huggard, and G. Toso, "Design of aperiodic frequency selective surfaces for compact quasi-optical networks," in *Proc. EuCAP*, 2017.

[13] E. B. Tchikaya, A. Rashid, F. Khalil, H. Aubert, H. Legay, and N. J. G. Fonseca, "Multi-scale approach for the electromagnetic modeling of metallic fss grids of finite thickness with non-uniform cells," in *Asia Pacific Microwave Conf. (APCM)*, 2009.

[14] M. Zhou, O. Borries, and E. Jørgensen, "Design and optimization of a single-layer planar transmit-receive contoured beam reflectarray with enhanced performance," *IEEE Trans. Antennas Propag.*, vol. 63, no. 3, pp. 1247–1254, 2015.

[15] A. Ericsson, D. Sjöberg, G. Gerini, C. Cappellin, F. Jensen, P. Balling, N. J. G. Fonseca, and P. De Maagt, "A Contoured-Beam Reflector Satellite Antenna Using Two Doubly Curved Circular Polarization Selective Surfaces," *IEEE Trans. Antennas Propag.*, 2020 (Early Access).